



AFRL-RW-EG-TR-2023-378

Research in Visual Neuroethology

Laura E. Bagge

Marisa S. McDonald

University of Florida
207 Grinter Hall
Gainesville, FL 32611-5500

Martin F. Wehling

Air Force Research Laboratory
Munitions Directorate
101 West Eglin Blvd
Eglin AFB, FL 32542-5910

July 2023

Final

Controlled By: USAF AFRL/RW
Distribution Statement: A
POC:RWTC

DISTRIBUTION STATEMENT A – Approved for public release. Distribution is unlimited.

AIR FORCE RESEARCH LABORATORY, MUNITIONS DIRECTORATE
Air Force Materiel Command • United States Air Force • Eglin Air Force Base

NOTICE AND SIGNATURE PAGE

Using Government drawings, specifications, or other data included in this document for any purpose other than Government procurement does not in any way obligate the U.S. Government. The fact that the Government formulated or supplied the drawings, specifications, or other data does not license the holder or any other person or corporation; or convey any rights or permission to manufacture, use, or sell any patented invention that may relate to them.

This report is the result of contracted fundamental research deemed exempt from public affairs security and policy review in accordance with SAF/AQR memorandum dated 10 Dec 08 and AFRL/CA policy clarification memorandum dated 16 Jan 09. This report is available to the general public, including foreign nationals. Copies may be obtained from the Defense Technical Information Center (DTIC) (<http://www.dtic.mil>).

AFRL-RW-EG-TR-2023-378 HAS BEEN REVIEWED AND IS APPROVED FOR PUBLICATION IN ACCORDANCE WITH ASSIGNED DISTRIBUTION STATEMENT.

FOR THE DIRECTOR:

Signed

MARTIN WEHLING, DR-04, DAF
Work Unit Manager, Computational
Engineering Sciences Branch

Signed

CALVIN ROMAN, DR-04, DAF
Science & Technical Advisor
Computational Engineering
Sciences Branch

This report is published in the interest of scientific and technical information exchange, and its publication does not constitute the Government's approval or disapproval of its ideas or findings.

REPORT DOCUMENTATION PAGE			<i>Form Approved OMB No. 0704-0188</i>		
Public reporting burden for this collection of information is estimated to average 1 hour per response, including the time for reviewing instructions, searching existing data sources, gathering and maintaining the data needed, and completing and reviewing this collection of information. Send comments regarding this burden estimate or any other aspect of this collection of information, including suggestions for reducing this burden to Department of Defense, Washington Headquarters Services, Directorate for Information Operations and Reports (0704-0188), 1215 Jefferson Davis Highway, Suite 1204, Arlington, VA 22202-4302. Respondents should be aware that notwithstanding any other provision of law, no person shall be subject to any penalty for failing to comply with a collection of information if it does not display a currently valid OMB control number. PLEASE DO NOT RETURN YOUR FORM TO THE ABOVE ADDRESS.					
1. REPORT DATE (DD-MM-YYYY) 07072023		2. REPORT TYPE Final		3. DATES COVERED (From - To) 30 Mar 2019 – 31 July 2023	
4. TITLE AND SUBTITLE Research in Visual Neuroethology			5a. CONTRACT NUMBER FA8651-19-F-1012		
			5b. GRANT NUMBER N/A		
			5c. PROGRAM ELEMENT NUMBER 62602F		
6. AUTHOR(S) Bagge, Laura E. McDonald, Marisa S.			5d. PROJECT NUMBER 2068		
			5e. TASK NUMBER 9951		
			5f. WORK UNIT NUMBER W17P		
7. PERFORMING ORGANIZATION NAME(S) AND ADDRESS(ES) University of Florida Office of Engineering Research 207 Grinter Hall Gainesville, FL 32611-5500			8. PERFORMING ORGANIZATION REPORT NUMBER N/A		
9. SPONSORING / MONITORING AGENCY NAME(S) AND ADDRESS(ES) Air Force Research Laboratory Munitions Directorate 101 West Eglin Blvd. Eglin AFB, FL 32542-6810			10. SPONSOR/MONITOR'S ACRONYM(S) AFRL/RWTC		
			11. SPONSOR/MONITOR'S REPORT NUMBER(S) AFRL-RW-EG-TR-2023-378		
12. DISTRIBUTION / AVAILABILITY STATEMENT DISTRIBUTION STATEMENT A – Approved for public release. Distribution is unlimited.					
13. SUPPLEMENTARY NOTES DISTRIBUTION STATEMENT INDICATING AUTHORIZED ACCESS IS ON THE COVER PAGE AND BLOCK 12 OF THIS FORM. DATA RIGHTS RESTRICTIONS AND AVAILABILITY OF THIS REPORT ARE SHOWN ON THE NOTICE AND SIGNATURE PAGE.					
14. ABSTRACT The Nature-Inspired Team in AFRL/RW is investigating biological systems for inspiration for novel high performance efficient approaches to the sensors, information processing, and systems architectures for guidance, navigation, and control to enable autonomous agents in GPS-denied environments. A specialist in vision neuroethology in arthropods is required to assist the government team working in RW's Natural Systems Sensing Laboratory, to investigate natural vision systems and the details of their design and its relation to the behavior of the animals in their natural environments.					
15. SUBJECT TERMS visual neuroethology; spectral vision; polarization vision; elementary motion detection; acuity; resolution					
16. SECURITY CLASSIFICATION OF:			17. LIMITATION OF ABSTRACT SAR	18. NUMBER OF PAGES 20	19a. NAME OF RESPONSIBLE PERSON Martin F. Wehling
a. REPORT Unclassified	b. ABSTRACT Unclassified	c. THIS PAGE Unclassified			19b. TELEPHONE NUMBER (850) 883-1880

Standard Form 298 (Rev. 8-98)
Prescribed by ANSI Std. Z39.18

TABLE OF CONTENTS

Section	Page
List of Figures	V
Introduction	1
1 Laura Bagge; Summary of Research.....	1
2 Marisa McDonald; Summary of Research	4
3 Publication.....	5
APPENDIX – A	A-1

LIST OF FIGURES

	Page
Laura Bagge Research	
Figure 1	Left-hand circularly polarized light (LHCP) is seen through the left LHCP lens and right-hand circularly polarized light (RHCP) is seen through the right RHCP lens 2
Figure 2	Diagram of the spectropolarimeter used to characterize the complete optical signatures from the beetle cuticles by measuring the spectral Mueller matrices 2
Figure 3	Plots of the degree of circular polarization (DOCP) calculated from spectral Mueller matrix element measurements taken of 5 species of golden scarab beetles to show the difference in polarization signatures 3
Marisa McDonald Research	
Figure 1	Close up images of the compound eyes and ocelli of (1) Blue bottle fly (<i>Calliphora vomitoria</i>), (2) Black Soldier Fly (<i>Hermetia illucens</i>), and a (3) Carpenter Ant (<i>Camponotus floridanus</i>) 5
Figure 2	Example spectral sensitivity curves obtained from the flying carpenter ant, in both the compound eye and ocellar structures..... 6

Introduction: UF FLA REEF abbreviated task description, Research in Visual Neuroethology (FA8651-19-F-1012)

The Nature-Inspired Team in AFRL/RWW is investigating biological systems for inspiration for novel high performance efficient approaches to the sensors, information processing, and systems architectures for guidance, navigation, and control to enable autonomous agents in GPS-denied environments. To this end, AFRL/RW maintains the Natural Systems Sensing Laboratory (NSSL), at this writing in building 8682 at Eglin AFB remote site C-86. The research in this lab emphasizes exploring the vision systems in natural systems that could provide relevant bases for advanced engineering sensors, as well as the associated behavior of these natural systems to understand the context and requirements flow among the environment, behavior, and design details of the systems.

A specialist in vision neuroethology in insects is required to assist the government team working in the NSSL, to investigate natural vision systems and the details of their design and its relation to the behavior of the animals in their natural environments. UF will provide a postdoctoral researcher dedicated to this task. UF anticipates the postdoc will work primarily in the NSSL, but UF will provide desk space at the UF REEF for the postdoctoral researcher.

The immediate objective of this task is to continue the development and operation of a vision neuroethology laboratory at AFRL/RW with a specific focus on understanding optical and information handling properties of natural vision systems. The NSSL will serve as the main location for experimental work. This work includes measuring optical signatures of animals and their corresponding visual sensitivities.

1. Laura Bagge: Summary of Research during Tenure as UFL Research Associate

During my tenure as a University of Florida Research Associate in the Natural Systems Sensing Laboratory at the Air Force Research Laboratory, I worked on questions related to the unique spectral and polarization optical signatures found in some insects that may serve to inspire improved designs of man-made sensors. I studied the underlying mechanisms for how insects may be able to perceive otherwise private channels, and my published work during my time as a UFL Research Associate may eventually lead to significant technological advancements for bioinspired target detection in engineered systems.

My original proposal included the goals of characterizing optical signatures produced by cuticular or wing structures in insects and then testing whether the insects can visually perceive those optical signatures (i.e., whether insects have neural matched filters for the visual wing signatures). I made the most progress in exploring circularly polarized light reflectance from scarab beetles and testing whether the beetles are sensitive to circularly polarized light signals. I have worked with my colleagues on the nature-inspired team to completely characterize the optical and polarization signatures from the wing surfaces of 50 different species of beetles, through measuring all spectral Mueller matrix elements. I published one paper (Bagge et al., *Applied Optics*, 2020) about the unusual optical signatures of five golden beetles that look alike to human vision but have different circularly polarized light reflectance properties. I have another paper in preparation about the signatures of the

other 50 species and what we can learn from this diversity of signals. Additionally, I have worked with my colleagues to better understand the ultrastructure of beetle eyes to determine how or if they are able to discriminate circularly polarized signals.



Figure 1. Left-hand circularly polarized light (LHCP) is seen through the left LHCP lens and right-hand circularly polarized light (RHCP) is seen through the right RHCP lens; because this gold beetle species strongly reflects LHCP but not RHCP, it appears different and the color is extinguished under the RHCP.

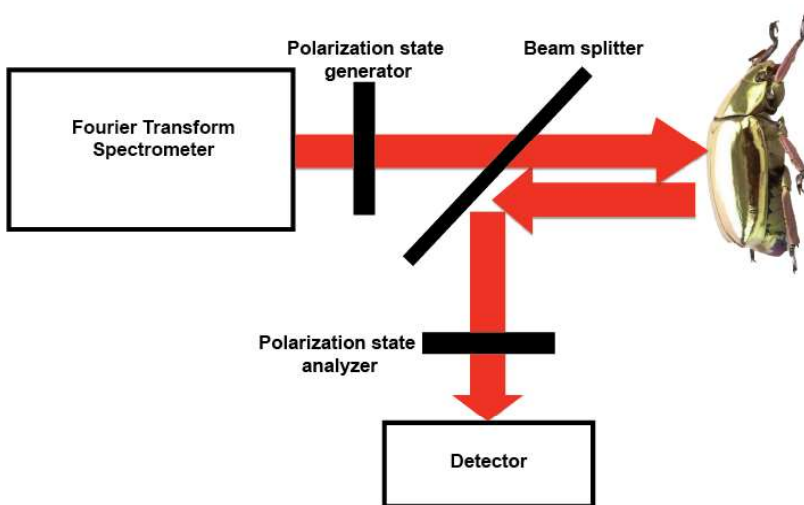


Figure 2. Diagram of the spectropolarimeter used to characterize the complete optical signatures from the beetle cuticles by measuring the spectral Mueller matrices.

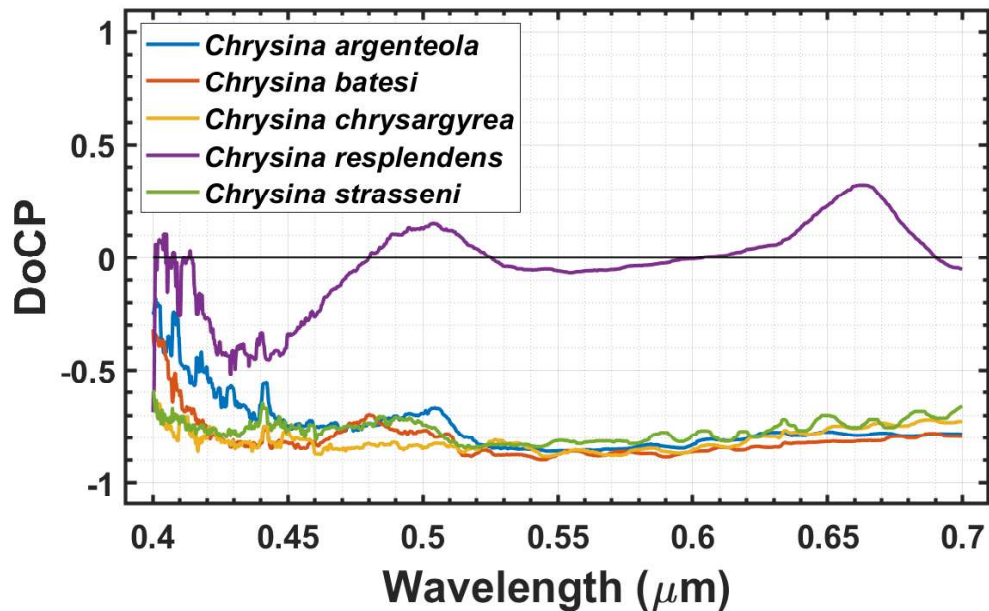


Figure 3. Plots of the degree of circular polarization (DOCP) calculated from spectral Mueller matrix element measurements taken of 5 species of golden scarab beetles to show the difference in polarization signatures. The conspicuous signature of *resplendens* suggests deeper analysis into the details of the signature generation is needed. Positive values are right-hand circularly polarized; negative values are left-hand circularly polarized.

Significant accomplishments during my tenure as an UFL Associate include:

- ~ One published paper (awarded Editor's Choice) in Applied Optics – Bagge, L.E., Kenton, A.C., Lyons, B.A., Wehling, M.F., and Goldstein, D.H. (2020). Mueller matrix characterizations of circularly polarized reflections from golden scarab beetles. *Applied Optics*. 59(21): F85-F93.
- ~Five technical presentations, including invited seminars and contributed conference papers.
- ~Two best presentation awards.
- ~Finally, data generated during my tenure as a UFL Research Associate can be used in future publications/patents by future postdocs in the lab, and I will continue to collect and analyze more related data in my current position as Senior Biologist, Insect Visual Systems at Torch Technologies.

Trips I took as a UF REEF research associate:

1) Light and Color in Nature Conference from July 14 to July 19 2019. Trip funded by NSF; presented a talk on the Wing Interference Patterns (WIPs) work and Circular Polarization in Beetles work.

2) International Conference on Invertebrate Vision IV, August 5 to August 12, 2019. Trip funded by UF REEF; presented a poster on the WIPs preliminary work.

3) MicroCT analysis course at Friday Harbor from August 25 to August 31 2019 (I was selected for the course, so lodging and course cost were covered, the REEF paid for flight to Seattle). The benefit to this course was to learn the analysis tools which I later applied to data collected at AFRL/RW's High Energy Research and Development facility (HERD).

4) Swiss Light Source from October 2 to October 10, 2019 (UF REEF paid for the flight, Mike Bok and Lauren Sumner-Rooney paid for the rest of the trip for me). The benefit to this was that I was able to scan the heads of beetles that Amanda Franklin sent to me, and these were the first data about their eye structures which we have shown on later posters.

2. Marisa McDonald: Summary of Research During Tenure as a University of Florida Postdoctoral Researcher

During my tenure as a postdoc working with the University of Florida and the Air Force Research Lab Nature Inspired team, I worked on questions related to the insect visual system, with focus on the secondary visual system many insects have, the ocelli (Figure 1). With this work I have investigated the physiology of visual systems, with an intention of better understanding what insects are able to see and how this translates into guided behavior. The goal of this work is to increase our understanding of relatively simple light detectors, like those of the ocelli, with the hope of inspiring new bioprincipic engineered systems.

My proposal for this work focused on characterizing the spectral and polarization sensitivity in the ocelli of a broad range of flying insects. In the 6 months that I was in this position, I assisted in setting up and optimizing an electroretinography rig in the lab that will be used to answer these questions. The equipment is now set up to be able to rapidly take measurements from live insect eyes to establish the temporal and spectral response of the eye. Preliminary testing on the equipment was completed on the ladybeetle species *Hippodamia convergens*. With these tests, we demonstrated that we can rapidly collect spectral sensing information from these insects. These insects were a useful test subject, as they are abundant, commercially available, and have commercial importance due to their impact on crops and gardens. We are currently working on a short publication on this visual system, as we have found no studies directly characterizing the ladybeetle eye of this species.

I have now begun preliminary studies on the insect ocellar system, working with two fly species: *Hermetia illucens*, the black soldier fly, and *Calliphora vomitoria*, the blue bottle fly, which can both be hatched and maintained in the lab environment. Recordings have also

been made on the flying carpenter ant *Camponotus floridanus* which was wild caught at the lab (preliminary results in Figure 2). This is an ongoing study in the lab, and we aim to gain insight into the ocellar sensitivities and compare across a broad range of groups.

In my tenure as a postdoctoral researcher, I had one publication accepted to the Journal of Crustacean Biology (reference below), which was featured on the cover of the journal issue. I also gave a presentation at the Society of Integrative and Comparative Biology annual conference (reference below). I am now working as an NRC Research Associate with the Air Force Research Lab Nature Inspired Team and will continue the work started as a UF postdoc moving forward.

Publication:

McDonald, M.S., Porter, M.L. (2023) Effect of light environment on prey consumption in two species of larval stomatopods, *Gonodactylaceus falcatus* (Forsk., 1775) and *Gonodactylillus* n. sp. (Stomatopoda: Gonodactylidae). Journal of Crustacean Biology. 43, 1-8.

Presentation:

McDonald, M.S., Cohen, J. H., Porter, M.L. 2023. Feeding Rates of Larval Stomatopods Under Different Light Environments. The Society of Integrative and Comparative Biology. Austin, Texas.



Figure 1: Close up images of the compound eyes and ocelli of (1) Blue bottle fly (*Calliphora vomitoria*), (2) Black Soldier Fly (*Hermetia illucens*), and a (3) Carpenter Ant (*Camponotus floridanus*). Red arrows point to the ocellar structures in the middle of the head for each.

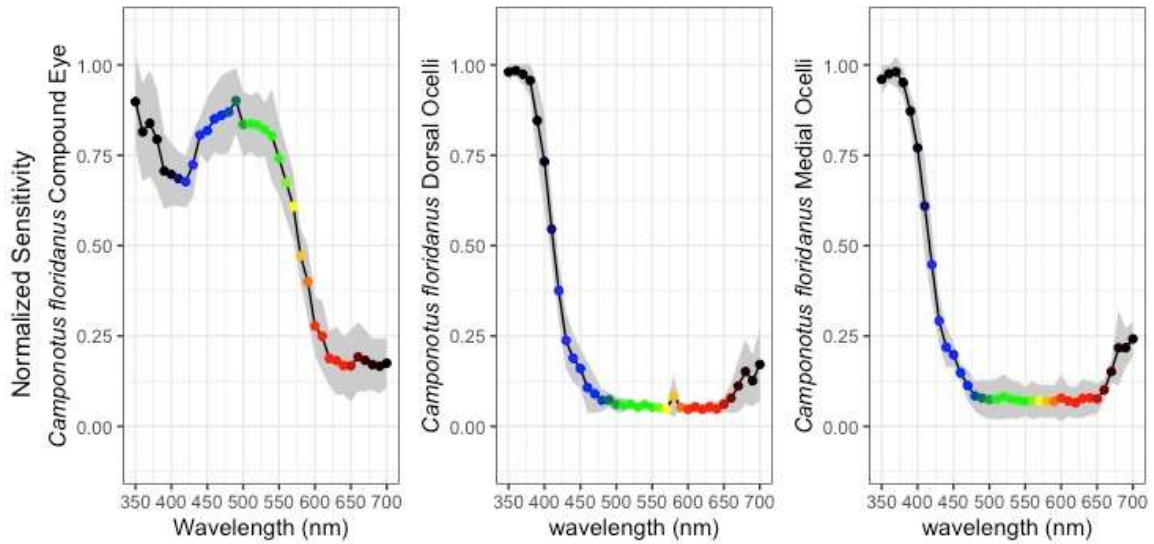


Figure 2: Example spectral sensitivity curves obtained from the flying carpenter ant, in both the compound eye and ocellar structures. There appears to be a small red sensitivity peak in the ocelli of this animal, which is noteworthy as Hymenoptera are not thought to have any red responses in the visual system.

Trip taken as a UF REEF research associate:

Society of Integrated and Comparative Biology annual meeting in Austin, TX, Jan 2023.



Mueller matrix characterizations of circularly polarized reflections from golden scarab beetles

Laura E. Bagge,^{1,2,3,*} Arthur C. Kenton,^{3,4} Bridget A. Lyons,^{3,5} Martin F. Wehling,³ and Dennis H. Goldstein³

¹National Resource Council Fellow of the National Academies of Sciences, Engineering, and Medicine, 500 Fifth St. N.W, Washington, DC 20418, USA

²University of Florida Department of Mechanical and Aerospace Engineering, 1350 Poquito Road N., Shalimar, Florida 32579, USA

³Air Force Research Laboratory/RWW, Eglin Air Force Base, Florida 32542, USA

⁴DCS Corporation, 109 Bailey Drive, Niceville, Florida 32578, USA

⁵Torch Technologies, Inc., 6 11th Ave. Suite F-1, Shalimar, Florida 32579, USA

*Corresponding author: laura.elizabeth.bagge@gmail.com

Received 28 May 2020; accepted 16 June 2020; posted 23 June 2020 (Doc. ID 398832); published 10 July 2020

Circularly polarized light (CPL) reflections are rare in nature. Only a few animal groups—most notably certain stomatopod crustaceans and certain beetles in the family Scarabaeidae—are known to reflect CPL from incident unpolarized light. Here, we examine five species of metallic scarabs in the genus *Chrysina* that, to the naked human eye, look remarkably similar. Using a spectropolarimetric reflectometer to characterize the complete Mueller matrix elements of the beetles' elytral surfaces, we found that four of the five species were strongly left-handed circularly polarized (LHCP), and only one scarab species, *Chrysina resplendens*, had an overall lower degree of polarization and switched from LHCP to right-handed circularly polarized reflectance depending on wavelength. © 2020 Optical Society of America

<https://doi.org/10.1364/AO.398832>

1. INTRODUCTION

Scarab beetles in the genus *Chrysina* (Coleoptera: Rutelinae: Scarabaeidae) have been prized for centuries due to their shiny, jewel-like appearance, and more recently have served as inspiration for biomimetic applications related to structural color [1–8]. These jewel scarabs (not to be confused with jewel beetles in the Buprestidae family) recently underwent a taxonomic revision in which the former genus *Plusiotis* was reclassified as the genus *Chrysina* [9], derived from the Greek word *chrysos* meaning gold. Not only do many of these *Chrysina* beetles have mirror-like golden surfaces, they also demonstrate the rare optical phenomenon of reflecting circularly polarized light (CPL). Ever since the discovery that the golden scarab beetle, *Chrysina resplendens*, reflects CPL [10], there has been interest in understanding how widespread this phenomenon is and what features of the cuticle contribute to CPL reflectance.

Interestingly, most *Chrysina* beetles examined thus far are known to strongly reflect left-handed circularly polarized (LHCP) light [11], but Michelson first noted that *C. resplendens* also reflected right-handed circularly polarized (RHCP) light [10]. The helicoidal layers in the cuticle responsible for the CPL reflectance have since been identified [7,12,13]. *C. resplendens* is unique thus far among other studied species in the *Chrysina* genus because its cuticle has two left-handed helicoidal regions,

separated by a unidirectional layer of birefringent material that acts as a half-wave plate retarder [12,14]. Over a certain wavelength range, this arrangement results in RHCP traveling through the first helicoidal layer, followed by a switch to LHCP upon the first transmission through the unidirectional retarder layer, then reflection by the second helicoidal layer, and then a switch back to RHCP reflectance on the return path through the unidirectional layer [12,14].

Even though transmission electron microscopy has revealed the ultrastructure of the cuticle of several specimens of *C. resplendens* that results in CPL, we still lack a complete understanding of how these chirped helical layers affect CPL signatures. Different studies have reported wide variations in the handedness and spectral response of CPL reflections in *C. resplendens* [11,15–21]. Some of these variations are the result of differing methods for measuring the CPL reflectances. For example, Hegedüs *et al.* used imaging polarimetry to characterize whole specimens of *C. resplendens* and other scarabs at blue, green, and red wavelengths [15]. Pye examined how widespread the phenomenon of CPL reflectance is in many groups of scarabs including *C. resplendens*, but this study did not distinguish wavelength-dependent effects [11]. Hodgkinson *et al.* [16] used ellipsometry methods to determine that the Mueller matrices for *C. resplendens* correspond with both right-circular and left-circular polarizers in the 400 to 900 nm

wavelength range. Fernández del Río [17] and Arwin *et al.* [18] also conducted Mueller matrix spectroscopic ellipsometry, but their small ($<100\ \mu\text{m}$) spot size and high angle of incidence (between 25° and 75°) relative to the surface plane measurements may not give us information about what another beetle or predator or prey may see as compared to Mueller matrix measurements that average over the entire elytral surface of the beetle. Additionally, Mendoza Gálvan *et al.* later used data measured from electron microscopy images (which may be influenced by tissue shrinkage that occurs during preparation) to model an expected Mueller matrix for *C. resplendens*, and showed RHCP reflectance peaking at over $800\ \text{nm}$ [19] as compared to Goldstein's measured Mueller matrix that showed RHCP peaking at approximately $600\ \text{nm}$ [20,21].

Because studies have suggested that certain metallic or golden beetles besides *C. resplendens* may also have wavelength-dependent CPL reflectance that may switch handedness, our study aims to further characterize these polarization properties, such as degree of polarization, handedness, and ellipticity, in additional species of scarab beetles. Our study is the first direct follow up to Goldstein's study [21] using the same spectropolarimetric reflectometer to measure the complete Mueller matrices of five species of golden scarabs (all from similar habitats in mountainous forests in Central America). While *C. resplendens* is arguably the beetle species that has received the most attention in the past and is included in this current study, we also include an additional four golden species that have never been measured before with this spectropolarimetric reflectometer method. By taking measurements that average over the entire elytral surface at normal incidence, we can compare our results with those obtained from ellipsometry methods and with those studies that characterize handedness based on viewing the beetles through polarizing filters in order to gain new insights into any ecological relevance of these polarization signatures.

2. EXPERIMENTAL DETAILS

A. Specimens

Spectral Mueller matrices were measured of five species of golden scarab beetle in the genus *Chrysina*: *Chrysina argenteola* [22], *Chrysina batesi* [23], *Chrysina chrysargyrea* [24], *Chrysina resplendens* [23], and *Chrysina strasseni* [25]. These beetle specimens were obtained on loan from the Florida State Collection of Arthropods in Gainesville, Florida, and had originally been collected in cloud forests in Costa Rica, Colombia, or Guatemala [26]. While we only report the complete Mueller matrices for one individual from each of the five species, we additionally report the Mueller matrices from eight specimens of a species previously measured by Goldstein, *Chrysina gloriosa* [9,27], to estimate the amount of variability that can exist within a single species. All beetle specimens were photographed using a Canon EOS 40D digital camera, with no polarizing filter initially, and then subsequently using a RHCP filter prior to the specimen being mounted and aligned in the spectropolarimetric reflectometer (Fig. 1).

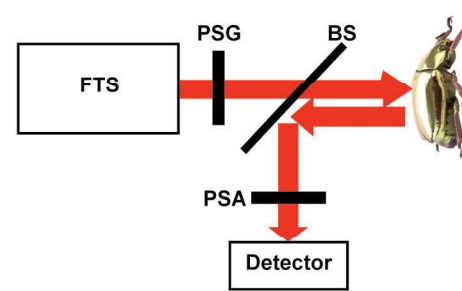


Fig. 1. Spectropolarimetric reflectance measurement configuration. FTS is the Fourier transform spectrometer, PSG is the polarization state generator, BS is the beam splitter, and PSA is the polarization state analyzer. The red arrows represent the light beam (that is larger than the beetle) hitting the dorsal curved surface of the beetle sample at normal incidence in this lateral view.

B. Dual Rotating Retarder Mueller Matrix Spectropolarimetric Reflectometer

The spectropolarimetric reflectometer used herein for Mueller matrix measurements is an instrument that measures spectral polarization properties of materials in transmission or reflection modes (Fig. 1). Its core is based on a commercial Fourier transform spectrometer (FTS), and it was previously described [28], patented [29], and used for precision measurements [20,21] for a variety of applications. For purposes of the measurements described here, the spectrometer is used with one source, an Oriel xenon lamp, and one silicon detector, such that the light collected is light that has been retroreflected at normal, or close to normal, incidence from the back of the beetles. Note that the light source has slightly lower intensity at shorter wavelengths, and the detector is also less responsive at shorter wavelengths. Together, these contribute to a lower signal and higher noise at shorter wavelengths compared to other wavelengths, as demonstrated in previous measurements [20,21,28]. The spectrometer serves as a radiation source for the polarimetric portion of the instrument and is operated in the conventional absorption spectroscopy mode. The radiation generated by the spectrometer is brought out through the spectrometer's external port.

Figure 1 shows the basic optical schematic of the instrument for monostatic reflectance measurements. The beetle sample was mounted vertically a short distance past the beam splitter (BS). The spot size was larger than any beetle specimen, which was pinned against a piece of black foam smaller than the beetle and so the beetle appeared suspended in air, such that any stray light that did not reflect off the dorsal surface of the beetle would go off several meters in the dark room to a beam dump and not be picked up by the detector. The optical system that collects light for the detector consists of an off-axis parabolic mirror. This mirror is oriented to look toward the beam splitter and to focus light on the detector that is mounted perpendicularly to the light coming from the beam splitter. The parabolic mirror, detector, and mounting devices form the detector assembly. The spectrometer was also used without any modification of the polarization of the source radiation (i.e., no added polarization elements). In this mode, it functions as a spectral reflectometer.

To obtain spectropolarimetric measurements, a dual rotating retarder Mueller matrix polarimeter, described by Azzam [30],

is included in the system. This polarimeter consists of a polarization state generator (PSG) before the sample and a polarization state analyzer (PSA) after the sample. The PSG consists of a linear polarizer followed by a quarter-wave retarder. The PSA consists of a quarter wave retarder followed by a linear polarizer in front of the detector assembly. Although achromatic retarders are used that were nominally quarter wave in the spectral region being measured, the exact retardance is not critical since errors in retardance from quarter wave are known from the calibration of the instrument and are compensated for during processing of the sample measurements (for complete calibration details, see [28,31]). When the retarders are rotated in a 5:1 ratio, all 16 elements of the sample Mueller matrix are encoded onto 12 harmonics of the detected signal; these are then Fourier analyzed to recover the Mueller matrix elements. Other previous implementations of this Mueller matrix polarimeter have been described elsewhere [32].

C. Theory and Calculations

The Mueller matrix formalism determines the reflected Stokes vector S_r in response to any incident Stokes vector S_i according to the equation

$$S_r = \mathbb{M}S_i, \tag{1}$$

where the Mueller matrix is

$$\mathbb{M} = \begin{pmatrix} m_{11} & m_{12} & m_{13} & m_{14} \\ m_{21} & m_{22} & m_{23} & m_{24} \\ m_{31} & m_{32} & m_{33} & m_{34} \\ m_{41} & m_{42} & m_{43} & m_{44} \end{pmatrix}, \tag{2}$$

where m_{21} is the linear polarizance in the horizontal/vertical, m_{31} is the linear polarizance at $\pm 45^\circ$, and m_{41} is the circular polarizance [33].

If unpolarized light illuminates the elytral surface of the beetles, our incident Stokes vector is

$$S_i = \begin{pmatrix} 1 \\ 0 \\ 0 \\ 0 \end{pmatrix}, \tag{3}$$

and therefore the reflected beetle Stokes vector is

$$S_r = \begin{pmatrix} m_{11} \\ m_{21} \\ m_{31} \\ m_{41} \end{pmatrix}. \tag{4}$$

By making spectral measurements using the spectropolarimetric reflectometer, all Mueller matrix elements are wavelength dependent and span visible wavelengths from 0.4–0.7 μm . This permitted us to calculate spectral polarization-related metrics. We determined the polarization state and degree as a function of wavelength. These results showed the amount of circular polarization reflected from the entire elytral surface of the beetle was wavelength dependent. More specifically, and similar to Arwin *et al.*'s study [18], we calculated the spectral degree of polarization (circular and linear) and the spectral ellipticity. Again, assuming unpolarized light illuminates the surface, these parameters of reflected light are

$$\text{Degree of Circular Polarization, or DoCP} = m_{41}, \tag{5}$$

$$\text{Degree of Polarization, or DoP} = \sqrt{m_{21}^2 + m_{31}^2 + m_{41}^2}, \tag{6}$$

and

$$\text{Degree of Linear Polarization, or DoLP} = \sqrt{m_{21}^2 + m_{31}^2}. \tag{7}$$

Equations (5)–(7) combine to show that the square of the degree of total polarization is equal to the sum of the squares of the degree of linear polarization and degree of circular polarization, or

$$\text{DoP}^2 = \text{DoLP}^2 + \text{DoCP}^2. \tag{8}$$

This relationship is useful for interpreting some of the results presented in the next section.

The ellipticity of the polarization ellipse is given by

$$e = \tan \left(\frac{1}{2} \sin^{-1} \left(\frac{m_{41}}{\sqrt{m_{21}^2 + m_{31}^2 + m_{41}^2}} \right) \right). \tag{9}$$

Pure LHCP light reflectance would have a DoCP (m_{41}) value and an ellipticity value of -1 , while the values for pure RHCP light reflectance would be $+1$. All polarization metrics were calculated from the raw unfiltered Mueller matrices (normalized to $m_{11} = 1$). The matrix elements were then smoothed along the wavelength axis using a median moving average filter (order 20). Additionally, the spectral reflectances of all beetles were measured using the same setup without polarization elements. The relative reflectance is normalized to the maximum spectral reflectance and smoothed using a median moving average filter (order 16). Thus, the reported reflectance measurements of the five beetle species are by necessity relative comparisons of the spectral peaks between species, since the spot size is larger than the beetles and the curved backs of the beetles, which are of different sizes, cannot be estimated as flat uniform panels.

3. RESULTS

A. Appearance Through CPL Filter

The five species of scarab beetles from the genus *Chrysina* examined in this study were chosen for their golden appearance and for comparison of their Mueller matrices to previously published results [15–21]. Photographs of these species without any polarizing filter (top row, Fig. 2) and through a RHCP filter (bottom row, Fig. 2) revealed that four of the five species showed a loss of color (becoming dark brown) through the RHCP filter. *C. resplendens* was the only beetle of these five that did not dramatically change appearance through the RHCP filter, as has also been shown in previous studies [15,21].

B. Reflectance

The spectral reflectances of the five species of beetles show similar reflectance peaks in the yellow to red part of the spectrum

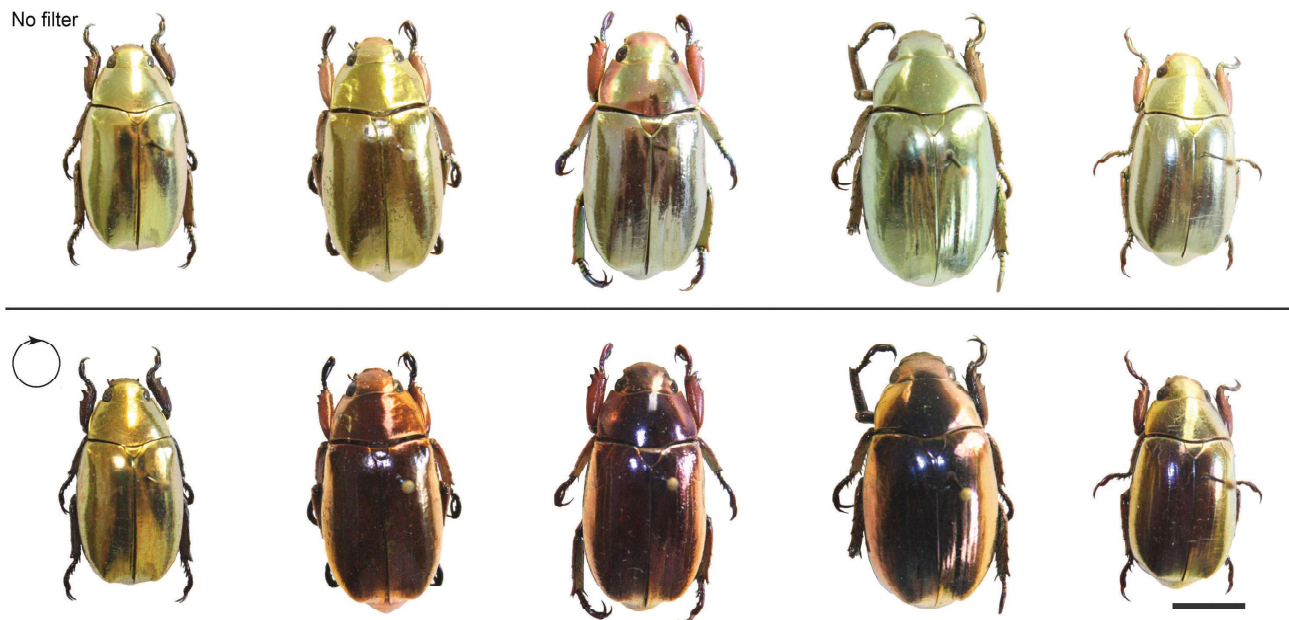


Fig. 2. Photographs of the five scarab species. The top row shows the beetles with no polarization filter. The bottom row shows the beetles through a RHCP filter. From left to right: *Chrysina resplendens*, *Chrysina argenteola*, *Chrysina chrysargyrea*, *Chrysina batesi*, and *Chrysina strasseni*. Scale bar is 10 mm.

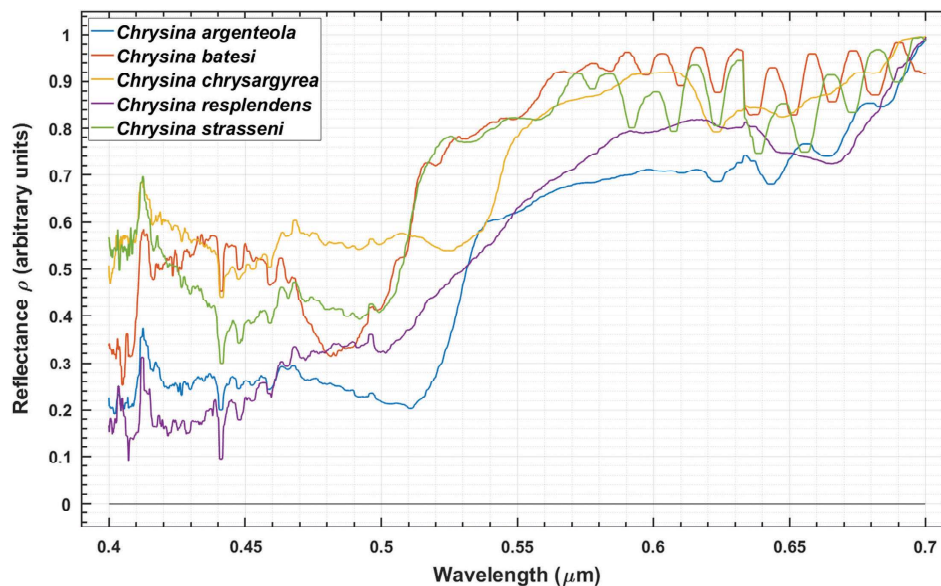


Fig. 3. Normalized reflectance spectra for the five golden beetle species at normal incidence.

that match with their “gold” appearance (Fig. 3). The oscillations indicate interference that is often seen in “metallic” colored animals that is a result of their cuticle structure [34,35]. As described in Section 2.C, these reported values are normalized values with arbitrary units, allowing for comparisons of spectral peaks, rather than absolute reflectance measurements (Fig. 3).

C. Mueller Matrix

The complete spectral Mueller matrix for *C. argenteola* is shown in Fig. 4 (see Fig. S1 for the other four species measured). *C. argenteola*, *C. chrysargyrea*, *C. batesi*, and *C. strasseni* were

all similar to Goldstein’s measurement of a different metallic (silver) species, *C. clypealis* [21]. *C. resplendens* was the only species out of the five examined that shows additional features in the Mueller matrix (Fig. S2 C). These are described in more detail along with other derived metrics below. Every gold species other than *C. resplendens* resembled a textbook Mueller matrix example of a wavelength-independent homogenous left-circular polarizer over most of the visible spectrum, i.e.,

$$\begin{pmatrix} 1 & 0 & 0 & -1 \\ 0 & 0 & 0 & 0 \\ 0 & 0 & 0 & 0 \\ -1 & 0 & 0 & 1 \end{pmatrix}.$$

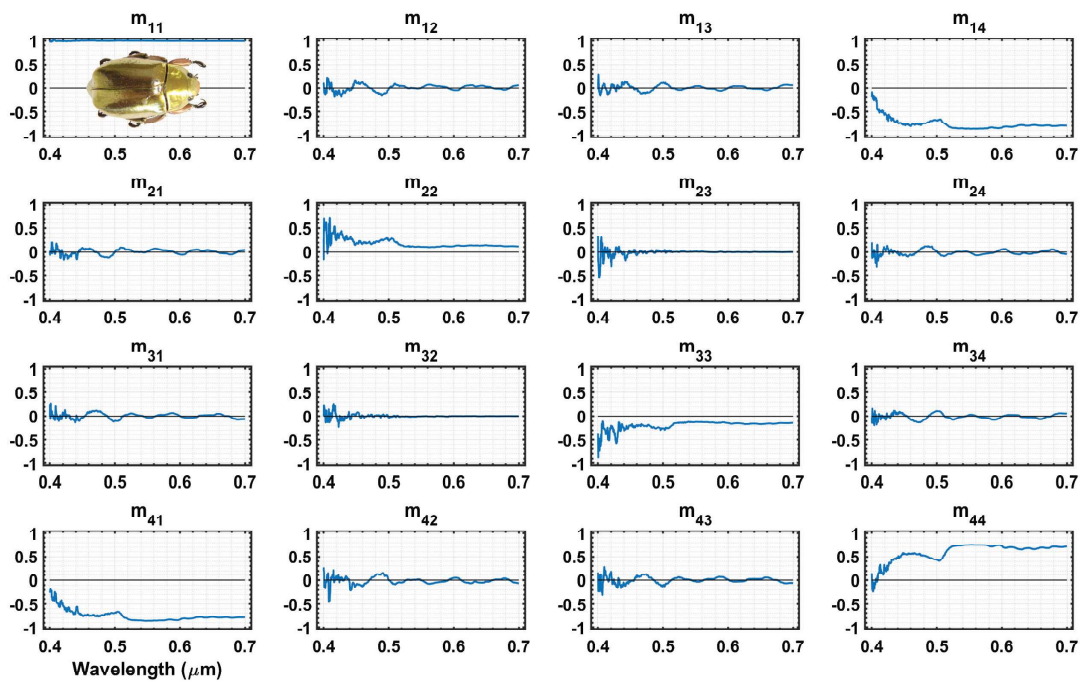


Fig. 4. Mueller matrix spectra for *C. argenteola* at normal incidence.

D. Left- and Right-Handedness and Other Polarization Parameters

First, to determine the amount of variability that can be found within one species of beetle, we measured the Mueller matrix and calculated derived metrics for eight specimens of *C. gloriosa*—a species previously reported in [21] (Fig. S2). Because overall variation between specimens of this species was

low (Fig. S2), the following results are reported only from a single specimen from each of the five golden species.

We explored derived metrics from the spectral Mueller matrix that are believed to be of biological significance: the degree of circular polarization (DoCP), ellipticity (ϵ), degree of polarization (DoP), and degree of linear polarization (DoLP) (Fig. 5). The DoCP is the element m_{41} . Values below zero indicate LHCP, and values above zero indicate RHCP. The ellipticity

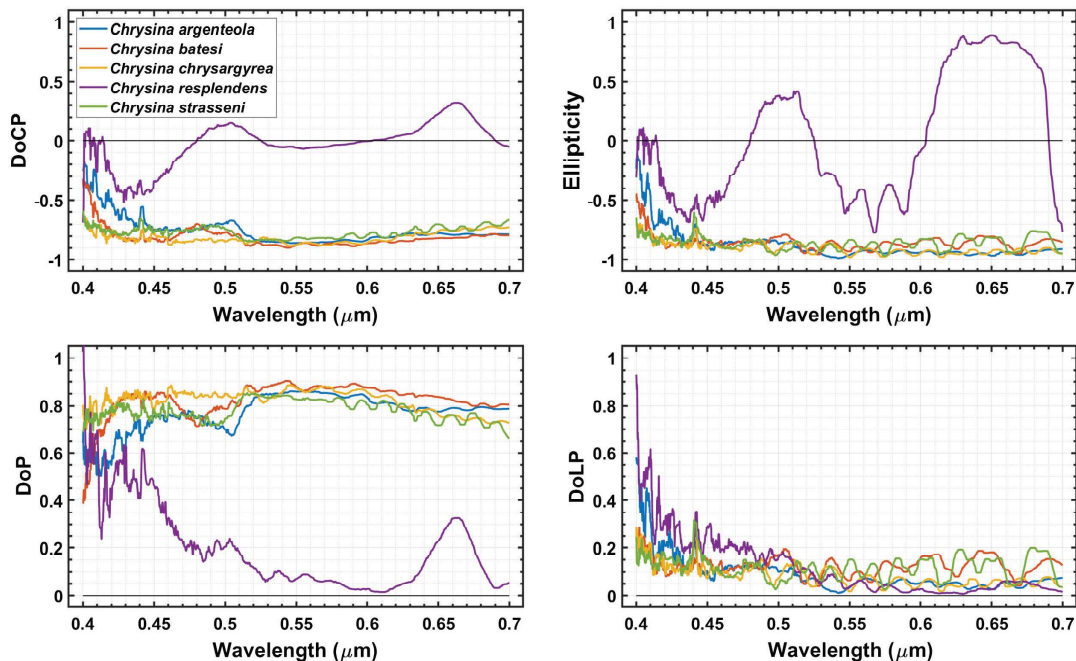


Fig. 5. Polarization metrics calculated from the Mueller matrices for the five species of beetles. Clockwise from top left: the degree of circular polarization (DoCP), ellipticity, degree of linear polarization (DoLP), and degree of polarization (DoP).

also tells us how circular the polarization is, with pure LHCP values at -1 and pure RHCP values at $+1$. While it may seem that DoCP and the ellipticity are closely related, there are cases where DoCP can be small but ellipticity is still close to one (pure circular). We must also consider how much of the total reflected light is polarized (DoP) which includes both DoCP and DoLP [see Eqs. (5)–(8)].

Four of the five beetle species showed similar signatures, with DoCP values between -0.7 and -0.9 and ellipticity values between -0.8 to -1.0 (Fig. 5). This indicates that these beetles were strongly LHCP spanning most of the visible spectrum. *C. resplendens* was the only species of the five that showed any wavelength-dependent shift to RHCP (Fig. 5).

C. resplendens showed LHCP from 400 to 480 nm, then switched to RHCP from 480 to 525 nm. Then there was another switch back to LHCP from 525 to 600 nm, and another switch to RHCP from 600 to 690 nm (Fig. 5). These wavelength-dependent switches in handedness are similar to what Goldstein [20,21] measured in a different *C. resplendens* specimen (see Fig. S3). During the first switch to RHCP (480–525 nm), the DoCP and ellipticity were approximately 0.15 and 0.4. During the second switch to RHCP (600–690 nm), the DoCP and ellipticity were approximately 0.33 and 0.9.

Interestingly, *C. resplendens* has a low DoP and low DoLP whereas the other four species have a very high DoP and low DoLP, consistent with their high “amount” of LHCP (where DOCP approaches -1). Referring to Eq. (8), *C. resplendens* shows a low DoLP and a low DoP, which must indicate low DoCP (i.e., closer to 0). The other four golden species show a low DoLP and a high DoP, which must indicate a high DoCP (i.e., closer to -1 in this case). Therefore, while *C. resplendens* does demonstrate RHCP, the overall DoP is very low relative to the other four species. This result is also consistent with the RHCP-filtered photographs (Fig. 2), where *C. resplendens* does not change appearance as dramatically as the other four species.

4. DISCUSSION

A. Reflectance and Polarization Properties of the Beetles

While the five species of golden scarabs examined in this study look similar to the naked human eye (Fig. 2), *C. resplendens* is clearly distinct from the other four species in several ways. Beginning with reflectance (Fig. 3), *C. resplendens* shows a more gradual reflectance increase spanning 500 to 600 nm. The other four species exhibit a “cuton” phenomenon at ~ 500 , 520, or 540 nm and show a rapid increase in reflectance over the 500 to 540 nm spectral range. *C. batesi* and *C. strasseni* appear to have the same “cuton” and show similar interference features at higher wavelengths (580 to 700 nm), suggesting a similar cuticle ultrastructure.

Our measurements of polarization properties further reveal that *C. resplendens* is unique among the metallic beetles measured. *C. argenteola*, *C. batesi*, *C. chrysargyrea*, and *C. strasseni* have a high, nearly constant, left-handed DoCP spanning most of the visible spectrum. Together, the DoCP and the ellipticity indicate the four species have a very high amount of DoCP of ~ -0.8 and ellipticity of ~ -0.9 . Since -1 for either of these metrics indicates pure LHCP, the four species are technically

elliptically polarized; however, they are approaching a full degree of circular polarization, and the ellipse is geometrically approaching a circle. In contrast, *C. resplendens* has a unique DoCP signature as compared to those other four species. The DoCP is relatively very low (~ -0.4 to 0.3) as compared to a near constant DoCP ~ -0.8 for the other four species. The DoCP spectrally shifts twice from left-hand elliptically polarized to right-handed elliptically polarized. This spans an ellipticity from -0.75 (left-hand elliptical) to $+0.4$ and $+0.9$ (right-hand elliptical) as a function of wavelength. The *C. resplendens* is the only beetle observed in our study that exhibited these properties. There are slight differences in the measurement results between the *C. resplendens* specimen measured in this study and a different individual measured in 2006 by Goldstein [21]. These differences can likely be explained by nutritional or environmental conditions that affect the exact composition of the cuticle (Fig. S3). The overall trend of the switch between LHCP and RHCP is demonstrated in both specimens (Fig. S3).

These spectral transits of *C. resplendens* into the RHCP regime add to the total DoP. This is prominently noted by a large spectral DoP feature approaching 0.33 at 663 nm and one of lesser prominence of 0.24 at ~ 500 nm. Additionally, *C. resplendens* has a slightly higher DoLP of 0.15–0.5 (400–500 nm) and a slightly lower DoLP of 0–0.1 (550–700 nm) as compared to the other four species. The other four species have a very low DoLP of 0.05–0.20 spanning the entire visible spectral region. For low DoLPs, the total DoP will be dominated by the behavior of the DoCP.

B. Comparison of Methods for Determining Mueller Matrices in Beetles

While we have not yet performed transmission electron microscopy to examine the ultrastructure of the cuticle of these five particular specimens, other studies have examined *C. resplendens* [12,14] and *C. chrysargyrea* [7] as well as other LHCP species of scarabs [13]. Based on our Mueller matrix measurements, we expect that the four specimens of *C. argenteola*, *C. batesi*, *C. chrysargyrea*, and *C. strasseni* have similar cuticle architecture and that *C. resplendens* is the only golden species with a different structure that consists of a birefringent layer that is sandwiched between two helicoidal layers. Interestingly, while we can use measured Mueller matrices to infer characteristics of the cuticle ultrastructure, we suggest that going in the opposite direction or using ultrastructure measurements alone to infer the Mueller matrix may result in inaccurate spectral peaks for both LHCP and RHCP reflectances (e.g., as reported by [19]). This may be due to the fact that exact thickness of layers in the cuticle of beetle specimens (dead or alive) can be difficult to determine because of the shrinkage of tissues that occurs when preparing a specimen for examination using electron microscopy.

Additionally, visual observations in the past generally have declared the characteristic of LHCP or RHCP by use of a like polarizer without reference to the degree of left or right elliptical character [11,15]. Our work provides a quantitative assessment of the amount that these five species of golden scarab beetles are elliptically/circularly polarized. Importantly, our measurements of Mueller matrix spectra account for the optical signature of the entire dorsal surface of the beetle. Because beetles have curved

backs, “normal incidence” refers to the fact that the beam of light (larger than the beetle) is positioned normal to the entire specimen. Since Goldstein presented the first complete Mueller matrix data for three species of scarab beetles [21], several studies have relied on ellipsometry methods to obtain Mueller matrix spectra for different scarabs at oblique incidences, using a small spot size ($<100\ \mu\text{m}$) on the beetle’s elytral surface [16–18,36–39]. It is interesting that our measurements of *C. argenteola* at normal incidence differed significantly from Arwin *et al.*’s [18] ellipsometer measurements, which were collected at non-normal incidence. These ellipsometer measurements at specific angles are most valuable in the determination of the internal structure along with validated models based on physical measurements of the layered structures; however, they are not necessarily representative of what one sees on observation of the beetles through circular polarizers by eye or with photographic equipment, or what one measures with the spectropolarimetric reflectometer with the specimens reflecting light off the entire surface. Our measured DoCP for *C. argenteola* was close to -1 across most of the visible spectrum, quite different from Arwin *et al.*’s measured DoCP that, at angles above 45° , showed a switch from LHCP to RHCP values. At 65° , *C. argenteola* showed high RHCP DoCP values between $+0.6$ and $+0.8$ at wavelengths between 600 and 800 nm [18]. That the handedness can change depending on angle of incidence requires further investigation. In *C. resplendens*, for example, we expect that the optical pathlength through the wave retarder in the beetle elytra will not be the same at different angles.

C. Biological Significance

The above comparisons bring into question what ecologically relevant polarization signals can be determined from the various methods of measuring Mueller matrices in beetles. While ellipsometry measurements can certainly reveal information about the nanostructure of the beetle’s cuticle and other useful optical information, they may not be relevant for understanding what a beetle or its predators or prey would actually see when viewing another beetle against a leafy background in a montane forest canopy. The spectropolarimetric reflectometer is designed to approximate the polarization and reflection signatures that may be observed in a natural environment, such as in the case of a beetle flying above another beetle and looking down at its dorsal surface.

Currently, we have little to no information about whether any of these golden scarab beetles may be able to distinguish any CPL signature. Overall, CPL reflections are rare in nature. However, recently marine crustaceans called stomatopods have been shown to use CPL signals in communication [40]. In fact, these crustaceans are able to distinguish LHCP from RHCP [41]. Whether or not CPL is detectable or serves a visual function in beetles remains unclear. Brady and Cummings [42] claimed that the beetle *C. gloriosa*, a strongly LHCP beetle, is able to differentiate unpolarized light from CPL, but the beetle *C. woodi*, a more elliptically polarized beetle, was not able to differentiate CPL. This suggests that the degree of polarization and ellipticity may play an important biological role. However, this study did not eliminate brightness cues as a confounding factor. Miao *et al.* [43] showed that *Anomala copulenta* use green

cuticle-reflected light for mate choice, but this approach did not allow the effects of color and polarization to be separated. Blahó *et al.* [44] tested four different species of scarab beetles and found no evidence that they were attracted to CPL when feeding or looking for mates or conspecifics.

Our study shows that *C. resplendens* has a very low DoP and DoLP, whereas the other four species have very high DoP and low DoLP consistent with a “high toward the left” DoCP (approaches -1). Whether or not the DoP exhibited by any species of golden scarab is enough to be detectable by the beetles requires further investigation into their visual capabilities, including their spectral sensitivities. For example, most insects are not able to see red; yet, all the beetles we measured show spectral reflectance peaks in the yellow to red part of the spectrum, and the second switch to RHCP in *C. resplendens* takes place around 650 nm. It was recently shown that an increased level of specular reflection of leaf backgrounds contributes to the survival of a certain species of shiny iridescent beetle, *Sternocera aequisignata* [45]. The camouflage of this beetle’s iridescence is enhanced, at least according to human vision, by the beetle choosing glossier backgrounds [45]. Additionally, Feller *et al.* [46] suggested that the golden reflectors in *C. resplendens* illustrate that intrinsic polarization properties can function to improve the overall reflectivity of the structure. These findings beg the question about whether our studied scarab species are under selection to increase their golden reflectivity to appear camouflaged to predators but perhaps use circular polarization (which is highly unlikely to be seen by any bird or mammal predator) as a covert signal.

Exploring whether any scarab beetles are actually sensitive to CPL and whether their eyes possess any potential morphological mechanisms for detecting and analyzing CPL is an important next step before we can then address questions regarding whether circular polarization functions as a covert signal. Generally, *Chrysina* species are found to occur in sympatric assemblages [2]; thus, the need to distinguish between closely related species may be an important evolutionary driver to CPL reflectance patterns.

5. CONCLUSIONS

This study compared five species of golden scarabs that—to humans at least—look similar and that have overlapping habitat distributions in mountainous forests in Central America. Previously, individual studies have been undertaken to characterize one species, or compare a few species of different colors, or examine the Mueller matrices at specific high angles of incidence. We wanted to follow up on Goldstein’s 2006 study to further explore the polarization properties of these “gold bugs” to determine if a common feature of being a golden scarab is having circular polarization that switches handedness dependent on wavelength. We conclude that *C. resplendens* is the only golden scarab species known that demonstrates a switch from LHCP to RHCP dependent on wavelength. Our measurements account for the entire elytral surfaces of the beetles, which is representative of what another beetle or predator would see. We conclude that *C. resplendens* has different polarization signatures than the other golden scarabs we measured, and future work will

examine their eyes to determine if they can discriminate LHCP or RHCP light.

Funding. Air Force Office of Scientific Research (LRIR 19RWCOR110); U.S. Air Force Research Laboratory.

Acknowledgment. We thank the Florida Department of Agriculture and Consumer Services—Florida State Collection of Arthropods, and especially Head Curator Paul Skelley and Curator of Coleoptera Kyle Schnepf for the loan of the scarab beetles. We also thank Sönke Johnsen, Doeke Stavenga, Tom Cronin, and other anonymous reviewers for comments on earlier versions of this paper. This research was performed while LEB held a National Resource Council Research Associateship award at the U.S. Air Force Research Laboratory, Eglin Air Force Base, Florida. LEB collected data, analyzed data, and wrote the manuscript; ACK performed Mueller matrix metric calculations, graphs, and analyses; BAL collected data and assisted with data interpretation; MFW assisted with data interpretation; DHG built the spectropolarimetric reflectometer, collected data, analyzed data, and supervised the whole project. **Public Release** DISTRIBUTION A. Approved for public release. Distribution unlimited. 96TW-2020-0155.

Disclosures. The authors declare no conflicts of interest.

See [Supplement 1](#) for supporting content.

REFERENCES

1. A. R. Parker, D. R. McKenzie, and M. C. J. Large, "Multilayer reflectors in animals using green and gold beetles as contrasting examples," *J. Exp. Biol.* **201**, 1307–1313 (1998).
2. D. B. Thomas, A. Seago, and D. C. Robacker, "Reflections on golden scarabs," *Am. Entom.* **553**, 224–230 (2007).
3. T. Lenau and M. Barfoed, "Colours and metallic sheen in beetle shells—a biomimetic search for material structuring principles causing light interference," *Adv. Eng. Mater.* **10**, 299–314 (2008).
4. V. Sharma, M. Crne, J. O. Park, and M. Srinivasarao, "Structural origin of circularly polarized iridescence in jeweled beetles," *Science* **325**, 449–451 (2009).
5. D. E. Azofeifa, M. Hernández-Jiménez, E. Libby, A. Solís, C. Barboza-Aguilar, and W. E. Vargas, "A quantitative assessment approach of feasible optical mechanisms contributing to structural color of golden-like *Chrysina aurigans* scarab beetles," *J. Quant. Spectrosc. Radiat. Transfer* **160**, 63–74 (2015).
6. C. Q. Cook and A. Amir, "Theory of chirped photonic crystals in biological broadband reflectors," *Optica* **3**, 1436–1439 (2016).
7. W. E. Vargas, E. Avendaño, M. Hernández-Jiménez, D. E. Azofeifa, E. Libby, A. G. Solís, and C. Barboza-Aguilar, "Photonic crystal characterization of the cuticles of *Chrysina chrysargyrea* and *Chrysina optima* jewel scarab beetles," *Biomimetics* **3**, 30 (2018).
8. P. Bouchal, J. Kapitán, M. Konečný, M. Zbončák, and Z. Bouchal, "Non-diffracting light in nature: anomalously reflected self-healing Bessel beams from jewel scarabs," *APL Photon.* **4**, 126102 (2019).
9. D. C. Hawks, "Taxonomic and nomenclatural changes in *Chrysina* and a synonymic checklist of species (Scarabaeidae: Rutelinae)," *Occ. Pap. Consortium Coleopterorum* **4**, 1–8 (2001).
10. A. A. Michelson, "On metallic colouring in birds and insects," *Philos. Mag.* **21**(124), 554–567 (1911).
11. J. D. Pye, "The distribution of circularly polarized light reflection in the Scarabaeoidea (Coleoptera)," *Biol. J. Linn. Soc.* **100**, 585–596 (2010).
12. S. Caveney, "Cuticle reflectivity and optical activity in scarab beetles: the role of uric acid," *Proc. R. Soc. London B* **178**, 205–225 (1971).
13. L. T. McDonald, E. D. Finlayson, B. D. Wilts, and P. Vukusic, "Circularly polarized reflection from the scarab beetle *Chalcothea smaragdina*: light scattering by a dual photonic structure," *J. R. Soc. Interface* **7**, 20160129 (2017).
14. E. D. Finlayson, L. T. McDonald, and P. Vukusic, "Optically ambidextrous circularly polarized reflection from the chiral cuticle of the scarab beetle *Chrysina resplendens*," *J. R. Soc. Interface* **14**, 20170129 (2017).
15. R. Hegedüs, S. Gyözö, and H. Gábor, "Imaging polarimetry of the circularly polarizing cuticle of scarab beetles (Coleoptera: Rutelidae, Cetoniidae)," *Vis. Res.* **46**, 2786–2797 (2006).
16. I. Hodgkinson, S. Lowrey, L. Bourke, A. Parker, and M. W. McCall, "Mueller-matrix characterization of beetle cuticle: polarized and unpolarized reflections from representative architectures," *Appl. Opt.* **49**, 4558–4567 (2010).
17. L. Fernández del Río, *An Investigation of the Polarization States of Light Reflected from Scarab Beetles of the Chrysina Genus* (Linköping University, 2011).
18. H. Arwin, R. S. Magnusson, J. Landin, and K. Järrendahl, "Chirality-induced polarization effects in the cuticle of scarab beetles: 100 years after Michelson," *Philos. Mag.* **92**(12), 1583–1599 (2012).
19. A. Mendoza-Galván, K. Järrendahl, and H. Arwin, "Mueller matrix modeling of the architecture in the cuticle of the beetle *Chrysina resplendens*," *J. Vac. Sci. Technol. B* **37**, 062904 (2019).
20. D. H. Goldstein, "Reflection properties of Scarabaeidae," *Proc. SPIE* **5888**, 58880T (2005).
21. D. H. Goldstein, "Polarization properties of Scarabaeidae," *Appl. Opt.* **45**, 7944–7950 (2006).
22. H. W. Bates, "Insecta. Coleoptera," in *Part 2. Pectinicornia and Lamellicornia*, O. Salvin and G. F. du Cane, eds. (R. H. Porter, 1988), Vol. **II**, pp. 1–432.
23. A. Boucard, "Monographic list of the Coleoptera of the genus *Plusiotis* of America, north of Panama, with descriptions of several new species," *Proc. Zool. Soc. Lond.* 117–125 (1875).
24. A. Sallé, "Diagnose d'une nouvelle espèce de *Pelidnota* (*P. chrysargyrea*)," *Ann. Soc. Entomol. Fr.* **5**, 362 (1874).
25. F. Ohaus, "*Plusiotis strasseni* new sp.," *Senckenbergiana* **6**, 185–186 (1924).
26. M. R. Moore, M. L. Jameson, B. H. Garner, C. Audibert, A. B. Smith, and M. Seidel, "Synopsis of the pelidnotine scarabs (Coleoptera, Scarabaeidae, Rutelinae, Rutelini) and annotated catalog of the species and subspecies," *ZooKeys* **666**, 1–349 (2017).
27. J. L. LeConte, "Descriptions of new coleoptera collected by Thos. H. Webb, M. D., in the years 1850–1851 and 52, while secretary to the U. S. and Mexican boundary commission," *Proc. Acad. Nat. Sci. Philadelphia* **7**, 220–225 (1854).
28. D. H. Goldstein and D. B. Chenault, "Spectropolarimetric reflectometer," *Opt. Eng.* **41**, 1013–1020 (2002).
29. D. H. Goldstein, D. B. Chenault, and M. Owens, "Spectropolarimetric reflectometer," U.S. patent 6,618,145 (9 September 2003).
30. R. M. A. Azzam, "Photopolarimetric measurement of the Mueller matrix by Fourier analysis of a single detected signal," *Opt. Lett.* **2**, 148–150 (1978).
31. D. H. Goldstein and R. A. Chipman, "Error analysis of a Mueller matrix polarimeter," *J. Opt. Soc. Am. A* **7**, 693–7700 (1990).
32. D. H. Goldstein, "Mueller matrix dual-rotating retarder polarimeter," *Appl. Opt.* **31**, 6676–6683 (1992).
33. D. H. Goldstein, *Polarized Light*, 3rd ed. (CRC Press, 2011).
34. A. C. Neville, "Metallic gold and silver colours in some insect cuticles," *J. Insect Physiol.* **23**, 1267–1274 (1977).
35. A. C. Neville and S. Caveney, "Scarab beetle exocuticle as an optical analogue of cholesteric liquid crystals," *Biol. Rev.* **44**, 531–562 (1969).
36. A. T. Berlind, B. D. Johs, and K. Järrendahl, "Cuticle structure of the scarab beetle *Cetonia aurata* analyzed by regression analysis of Mueller-matrix ellipsometric data," *Opt. Express* **21**, 22645–22656 (2013).
37. H. Arwin, R. Magnusson, E. Garcia-Caurel, C. Fallet, K. Järrendahl, M. Foldyna, A. De Martino, and R. Ossikovski, "Sum decomposition of Mueller-matrix images and spectra of beetle cuticles," *Opt. Express* **23**, 1951–1966 (2015).

38. E. Muñoz-Pineda, K. Järrendahl, H. Arwin, and A. Mendoza-Galván, "Symmetries and relationships between elements of the Mueller matrix spectra of the cuticle of the beetle *Cotinis mutabilis*," *Thin Solid Films* **571**, 660–665 (2014).
39. R. S. Magnusson, H. Arwin, E. García-Caurel, K. Järrendahl, and R. Ossikovski, "Sum regression decomposition of spectral and angle-resolved Mueller matrices from biological reflectors," *Appl. Opt.* **55**, 4060–4065 (2016).
40. Y. L. Gagnon, R. M. Templin, M. J. How, and N. J. Marshall, "Circularly polarized light as a communication signal in mantis shrimps," *Curr. Biol.* **25**, 3074–3078 (2015).
41. T.-H. Chiou, S. Kleinlogel, T. Cronin, R. Caldwell, B. Loeffler, A. Siddiqi, A. Goldizen, and J. Marshall, "Circular polarization vision in a stomatopod crustacean," *Curr. Biol.* **18**, 429–434 (2008).
42. P. C. Brady and M. E. Cummings, "Differential response to circularly polarized light by the jewel scarab beetle *Chrysina gloriosa*," *Am. Nat.* **175**, 614–620 (2010).
43. J. Miao, Y. Wu, K. Li, Y. Jiang, Z. Gong, Y. X. Duan, and T. Li, "Evidence for visually mediated copulation frequency in the scarab beetle *Anomala corpulenta*," *J. Insect Behav.* **28**, 175–182 (2015).
44. M. Blahó, A. Egri, R. Hegedüs, J. Jósmai, M. Tóth, K. Kertész, L. Biro, G. Kriska, and G. Horváth, "No evidence for behavioral responses to circularly polarized light in four scarab beetle species with circularly polarizing exocuticle," *Physiol. Behav.* **105**, 1067–1075 (2012).
45. K. Kjernsmo, H. M. Whitney, N. E. Scott-Samuel, J. R. Hall, H. Knowles, L. Talas, and I. C. Cuthill, "Iridescence as camouflage," *Curr. Biol.* **30**, 551–555 (2020).
46. K. D. Feller, T. M. Jordan, D. Wilby, and N. W. Roberts, "Selection of the intrinsic polarization properties of animal optical materials creates enhanced structural reflectivity and camouflage," *Phil. Trans. R. Soc. B* **372**:20160336 (2017).